Journal of Heat and Mass Transfer Research

Journal homepage: https://jhmtr.semnan.ac.ir

Semnan University

ISSN: 2383-3068

Research Article

CFD Analysis on the Performance of Twisted Tapes in Horizontal Heat Exchangers for Shower Water Heat Recovery

Eduardo Silva [a], Vitor Ferreira [b], José Cunha [b], Eliseu Monteiro [a,b] *

[a] *Faculty of Engineering, University of Porto, Rua Dr. Roberto Frias, 4200-465 Porto, Portugal*

[b] *LAETA-INEGI, Associated Laboratory for Energy, Transports and Aeronautics- Institute of Science and Innovation in Mechanical and Industrial Engineering, Rua Dr. Roberto Frias, 4200-465 Porto, Portugal*

ARTICLE INFO

Article history:

Received: 2024-09-04

Revised: 2024-10-31

Accepted: 2024-11-19

Keywords:

Computational fluid dynamics;
Convection;
Energy sustainability;
Wastewater heat exchanger;
Twisted tape.

ABSTRACT

The thermal energy found in shower hot wastewater, which is usually dumped, can be recovered through heat exchangers and used to pre-heat shower cold-water, contributing to energy sustainability. The objective and novelty of this work are to present a computational fluid dynamics (CFD) model and a theoretical model based on literature correlations to evaluate the performance of a shower water horizontal heat exchanger with twisted tape inserts. CFD simulations are used to improve the shape of twisted tape in the setting of the turbulator. The findings suggest that the wastewater flow convection heat transfer coefficient is between the flow around a cylinder and the flow around a cylinder in a narrow channel. The results for the turbulator are consistent with theoretical data, except for twist ratios below 3. The most promising twisted tape design has a twist ratio of 4 and a thickness of 1 mm. A conclusion could be drawn that the efficacy of the twisted tape in the heat exchanger is greater at lower flow rates. The performance gain ranges from 18.1 % to 3.0 % for flow rates of 3–10 L/min. Future directions for this research should focus on the improvement of the external convection coefficient because it represents the highest thermal resistance in the shower wastewater horizontal heat exchanger.

1. Introduction

Energy sustainability and the effects of climate change on civilization are currently among the key areas of scientific study. By creating new clean energy sources, clean technology, and increased energy efficiency, the goal is to lessen the negative effects of human activity [1]. Natural gas is widely used for water heating across the world, and it contributes significantly to greenhouse gas emissions from dwellings. As a result, lowering the energy required for water heating is critical to minimizing the use of fossil fuels, particularly considering global warming. One of the subjects under investigation in this area is the recovery of energy carried by wastewater, which has previously been acknowledged by the European Parliament as a renewable energy source [2, 3]. Showers provide a fantastic chance to recover wastewater heat by employing heat exchangers to preheat the flow of cold-water [4]. This saves energy while heating cold-water, reducing the requirement for outside sources of energy [5]. Multiple types of heat exchangers can be built beneath the shower to recover the heat from hot wastewater. They may be classified as heat exchanger-integrated showers, horizontal heat

* **Corresponding author.**
E-mail address: emonteiro@fe.up.pt

Cite this article as:

Silva, E., Ferreira, V., Cunha, J. and Monteiro, E., 2025. CFD Analysis on the Performance of Twisted Tapes in Horizontal Heat Exchangers for Shower Water Heat Recovery. *Journal of Heat and Mass Transfer Research*, 12(1), pp. 137-150.

https://doi.org/10.22075/JHMTR.2024.35215.1604

exchangers, or vertical heat exchangers [6]. Research indicates that vertical heat exchangers exhibit superior effectiveness compared to horizontal ones [7]. Shields [8] showed a decrease in effectiveness from 67% to 17% while switching from a vertical to a horizontal heat device. Wong et al. [9] obtained effectiveness in the range of 5-15 % when performing experimental work on horizontal heat exchangers in an apartment building. Many residences lack the necessary room to install vertical shower heat exchangers despite their better effectiveness [1]. Consequently, Kordana-Obuch et al. [10] conducted a survey of a sample of 462 inhabitants in Poland, revealing considerably larger potential recipients of horizontal devices compared to the potential recipients of vertical ones. Besides effectiveness, the payback period is a key factor when trying to get people to adopt this solution. Studies showed that the payback period can range from 2 years [7] to 13 years [13] or even beyond the technical lifetime of the system [5]. In general, the economic performance of these appliances improves with higher water usage and longer shower periods. These devices are ideal for use in swimming pools, gymnasiums, and health clubs [12]. Moreover, the research underlines the benefits of these components, not only in large buildings with significant water demand but also in private homes [6]. For these reasons, the focus of this research study on wastewater heat recovery by using horizontal heat exchangers should be the improvement of its effectiveness since it can cut energy usage and reduce costs.

Heat exchanger tubes are the primary components of a heat exchanger that transfer heat from a hot fluid to a cool fluid. Given the boundary layer's low heat transfer efficiency, the shape of the heat exchanger tube, which had a significant influence on boundary layer thickness, principally regulated the heat exchanger's thermo-hydraulic performance [13]. Integrating vortex generators or twisted tape inserts inside the tube has been employed to improve thermal performance. The tape or vortex generator placed into the tube can disrupt the fluid flow and diminish the boundary layer, hence improving heat transfer efficiency. Twisted tapes are metallic strips that have been twisted into a precise shape and dimension before being put across the flow. They are also considered swirl flow devices because they operate as turbulators to impart swirl flow, which increases the heat transfer coefficient. Varun et al. [14] evaluated research that investigated the effects of twisted tape inserts on the thermal performance of circular heat exchanger tubes. They concluded that using twisted tape in heat exchanger systems is a very effective means of enhancing heat transfer. The use of twisted tape inserts results in a gain in Nusselt number, friction factor, and thermal performance; however, this is accompanied by some pressure loss. Pitch and twist ratio are important criteria for evaluating the effectiveness of twisted tapes [14]. The pitch of a twisted tape is the distance between two locations in a plane parallel to the tape's axis, while the twist ratio is the pitch to the inner diameter of the tube. Various experimental and numerical studies on heat transfer enhancement utilizing twisted tapes have been conducted in recent years. Patil and Babu [15] investigated heat transfer enhancement in a circular tube and a square duct utilizing twisted and screw tape inserts. They found that using twisted and screw tapes for heat transfer intensification is a cost-effective approach. They also revealed that the increase in heat transfer in square ducts is greater than that in circular ducts due to the square duct's high surface-to-volume ratio. Sarma et al. [16] proposed a new approach for calculating the heat transfer coefficient in a tube with twisted tapes. The approach relied on a friction coefficient correlation to modify wall shear and temperature gradients, resulting in improved heat transfer through the tube wall. The resulting predictions were compared to several previously developed correlations for twisted tapes. Sarma et al. [17] developed universal correlations for convective heat transfer and friction coefficients in tubes with twisted tapes across various Prandtl and Reynolds values. A theoretical solution was presented for the Reynolds number range of 200–105 with a twist ratio of 2–10. They also gave generalized correlations for the Nusselt number and friction factor, with a variation of less than 12%. Yadav et al. [18] used CFD to simulate the thermohydraulic properties of a circular tube with twisted tapes. The average difference between predicted CFD findings and previously published experimental data for Nusselt number and friction factor was less than 9% [19]. In addition to the pressure loss and heat transfer, the friction factor, Nusselt number, and effectiveness of a tube with twisted tape inserts of different tape length ratios are computed. Their results show that the twisted tape tube with a variable tape length ratio works better thermo-hydraulically than the smooth tube. It was discovered that the tube with the full-length tape insert was more efficient. Shabanian et al. [20] examined the thermal performance, friction, and heat transfer characteristics of an air-cooled heat exchanger containing butterfly, classic, and jagged twisted tapes. The maximum thermal performance factor was obtained with butterfly inserts tilted at a 90° angle, according to the data. Moreover, the variation in heat transfer rates

between classic and jagged twisted tapes is lessened by lowering the twist ratio. The effects of turbulence were predicted by resorting to the RNG k-e turbulence model. For the Nusselt number and friction factor, good matches were realized between predicted and experimental data. Wang et al. [21] performed a numerical study utilizing CFD modeling to optimize the design of turbulent flow heat transfer for a circular tube with air serving as the working fluid and uniformly spaced twisted tape. The results show that in uniformly spaced short-length twisted tape, twist ratio is a significant influencing factor for flow resistance characteristics. The results showed that computational outcomes successfully supported experimental data. Higher heat transfer and flow resistance were attained with a bigger rotated angle.

Several other approaches have been proposed in the literature to improve heat transfer in heat exchangers. Jayranaiwachira et al. [22] investigated the entropy production and thermohydraulic performance of a uniform heat-flux tube fitted with louvered corner-curved baffle tape (LCBT). The results show that the LCBT with the smallest values of Prandtl = 1, θ = 0° yield the highest Nusselt and friction factor at roughly 4.4 and 19.2 times above the plain tube values. Using the LCBT at Prandtl = 1, θ=45° resulted in the highest thermal enhancement factor of approximately 2.23. The authors proposed Nusselt and friction factor empirical correlations for using LCBTs. Wang et al. [23] use a V-shaped fixed ring with perforated rectangular vortex generators to investigate the effect of their number, area, and pitch on heat transfer and pressure drop in turbulent circumstances. The results reveal that vortex number and area have consistent effects on heat transfer intensity and pressure drop, although the value of pitch is inversely related to both pressure drop and heat transfer intensity. Nakhchi and Esfahani [24] used numerical simulations to study the thermal performance of turbulent flow inside a heat exchanger tube with cross-cut twisted tape on an alternate axis. The results show that twisted tape has a stronger influence on heat transfer at lower inlet fluid velocities. The findings also indicate that increasing the twisted tape's width to diameter ratio improves thermal performance.

The current state of the art reveals that studies of the effect of twisted tape on the heat transfer of heat exchangers are scarce. It also reveals that the CFD technique has only been applied recently in this regard. Therefore, the main objective and novelty of this work is to provide theoretical and CFD results on the heat transfer of clean water flow in a shower's wastewater heat exchanger under the same cover. To simulate various geometries of twisted tape inserts, a 3D CFD model is used, resorting to Ansys Fluent. The remaining part of the paper is organized as follows: Section 2 presents the theoretical model implemented and the CFD model developed. Section 3 is divided into three subsections. Section 3.1 presents the results and discussion of the heat exchanger without twisted tapes using four theoretical models. Section 3.2 presents the results and discussion of the CFD simulations considering the heat exchanger with twisted tapes and presents a mesh quality study prior to the simulations. The main conclusions drawn from this study, the contribution to current knowledge, and some perspectives for its development are mentioned in Section 4.

2. Materials and Methods

2.1. Horizontal Heat Exchanger

The horizontal heat exchanger considered in this study is a prototype made up of twenty-five steel tubes that are joined by twenty-four plastic 180º elbows. Cold-water passes through the tubes, while hot water is contained inside a rectangular plastic shell. The set of cold-water tubes and the assembled prototype are depicted in Figure 1.

(a)

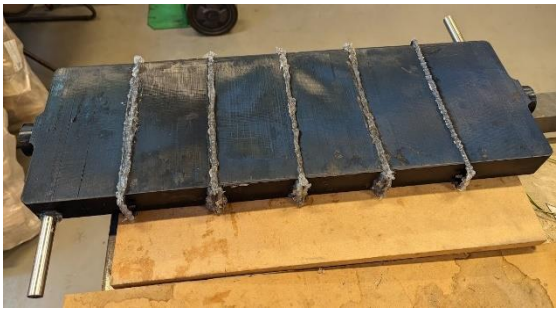

(b)

Fig. 1. Heat exchanger prototype: (a) Array of tubes and elbows; (b) Prototype assembled

The geometry of the heat exchanger used in the theoretical and CFD models is presented in Table 1. The diameters of the inner and outer tubes are denoted by d_i and d_o, respectively. The cold-water tube's center is located 9.5 mm above the shell's base. $l_{1,\,tube}$ denotes the length of the

steel tubes. The elbows form a semi-circle at the tube's center with a diameter of d_{elbow}. The variables b_{shell}, h_{shell}, and l_{shell} represent the dimensions of the internal section of the shell where hot water circulates.

Table 1. Dimensions of the heat exchanger

Column A	**[mm]**
Tube inner diameter (d_i)	13.8
Tube outer diameter (d_o)	15
Tube length (l_{tube})	135
Elbow diameter (d_{elbow})	24
Base of the shell (b_{shell})	196
Height of the shell (h_{shell})	38
Length of the shell (l_{shell})	616

According to NEN 7120:2011 [25], for computations and laboratory research, the boundary conditions for the cold-water inlet temperature is 10°C and the hot shower water temperature is 40°C. Equation (1) calculates the heat exchanger effectiveness (ε_{he}) for an adiabatic horizontal heat exchanger with equal mass flow rates and specific heat capacity of hot and cold water.

$$\varepsilon_{he} = \frac{T_{c,out} - T_{c,in}}{T_{h,in} - T_{c,in}} \tag{1}$$

$T_{c,in}$, $T_{c,out}$, $T_{h,in}$, and $T_{h,ou}$ denote the initial and final temperatures of the cold and hot flows, respectively. The range of mass flow rates was established between 3 and 10 L/min based on typical European shower head mass flow rates of 8-12 L/min [26], typical American shower flow rates of 7.9 L/min [27]. The overall heat transfer coefficient (U) is determined using Eq. (2) [28].

$$\frac{1}{U.A_{ht}} = \frac{1}{h_i.A_i} + \frac{\ln(d_o / d_i)}{2\pi.\lambda.l} + \frac{1}{h_o.A_o} \tag{2}$$

h_o and h_i stand for the average heat transfer convection coefficient for the hot and cold sides, respectively. A_{ht} denotes the area of heat transfer, while A_i and A_o represent the areas for inside and outside convection, respectively. λ stands for the wall thermal conductivity.

Equation (3) equates the two expressions for the heat transfer rate [28].

$$U.A_{ht}.\frac{(T_{h,out} - T_{c,in}) - (T_{h,in} - T_{c,out})}{\ln[(T_{h,out} - T_{c,in}) / (T_{h,in} - T_{c,out})]} = \dot{m}_c.c_{p,c}.(T_{c,out} - T_{c,in}) \tag{3}$$

Since Eq. (3) involves two unknowns, $T_{c,out}$, and $T_{h,out}$, Eq. (4) is introduced to provide a solution [28].

$$\dot{m}_h.c_{p,h}.(T_{h,out} - T_{h,in}) = \dot{m}_c.c_{p,c}.(T_{c,out} - T_{c,in}) \tag{4}$$

The heat exchanger's effectiveness may be computed after all temperatures have been obtained. $\dot{m}_c$, $c_{p,c}$, $\dot{m}_h$, and $c_{p,h}$ represent the mass flow rate and specific heat of the cold and hot flows, respectively. To calculate the overall heat transfer coefficient, the relevant correlations available in the literature are presented in the following subsections for cold and hot water flows.

2.1.1. Cold Water Heat Transfer Coefficient

For the flow rates under investigation, the cold-water flow through the pipe is turbulent. The length (l) considered for applying the correlations will be the same as that of the steel pipe, disregarding the elbow length. This happens because the elbows have a higher heat transfer resistance. Therefore, the walls of the elbow are regarded as adiabatic. Three distinct correlations are used and assessed to estimate the heat transfer coefficient. Equations (5) and (6), characterize the first correlation, which is dependent on the pipe's Reynolds number (Re), Prandtl number (Pr), inner diameter (d_i), and length (l). Equation (6) determines the ξ factor, which is used to determine the Nusselt number (Nu). It is applicable for Re between 10^4 and 10^6, Pr between 0.1 and 1000, and d_i/l less than or equal to 1 [29].

$$Nu = \frac{(\xi/8).\mathrm{Re}.\mathrm{Pr}}{1+12.7.\sqrt{\xi/8}.(\mathrm{Pr}^{2/3}-1)}[1+d_i/l)^{2/3}] \tag{5}$$

$$\xi = (1.8.\log_{10}\mathrm{Re}-1.5)^{-2} \tag{6}$$

In the second correlation (Equation (7)), the friction factor (f) is also considered. This correlation is valid for Re between 3000 and 5×10^6 and Pr between 0.5 and 2000 [28].

$$Nu = \frac{(f/8).(\mathrm{Re}-1000).\mathrm{Pr}}{1+12.7.\sqrt{f/8}.(\mathrm{Pr}^{2/3}-1)} \tag{7}$$

The friction factor is calculated using Haaland's equation (Equation (8)), where e_r is the equivalent roughness [30].

$$\frac{1}{\sqrt{f}} = -1.8.\log_{10}\left[\left(\frac{\varepsilon_r/d_i}{3.7}\right)^{1.11} + \frac{6.9}{\mathrm{Re}}\right] \tag{8}$$

The third correlation (Equation (9)), also known as one of the Dittus-Boelter equations, is valid for Re greater than 10000, Pr between 0.6 and 160, and l/d_i greater than or equal to 10 [28].

$$Nu = 0.0243.\mathrm{Re}^{4/5}.\mathrm{Pr}^{0.4} \quad (9)$$

2.1.2. Hot Water Heat Transfer Coefficient

In our prototype, hot shower water surrounds cold-water tubes in an empty channel with a rectangular section. Certain assumptions and approximations are required since this setup has not been documented in the literature. The heat exchanger's slope must be considered when calculating the flow height in the channel. Reducing bypassing by minimizing the water height above the tubes is crucial for optimal thermal performance. As a first engineering approximation, the water flow rate is taken to be around 2 mm above the tubes. Equation (10), which considers the water's crossflow around a cylinder, is used to determine the convection coefficient.

$$Nu = 0.0243.\mathrm{Re}^{4/5}.\mathrm{Pr}^{0.4} \quad (10)$$

The coefficients *C* and *m* are provided in Table 3. It is valid for *Pr* greater than or equal to 0.7 [28].

Table 3. Coefficients for the crossflow of water around a cylinder

Re	C	m
0.4-4	0.989	0.330
4-40	0.911	0.385
40-4000	0.683	0.466
4000-40000	0.193	0.618
40000-400000	0.027	0.805

If one considers crossflow around a cylinder but in a restricted channel, the Nusselt number can be calculated using Equation (11). It is valid for *Re* between 10 and 10^7 and *Pr* between 0.6 and 1000 [29].

$$Nu_{l,0} = 0.3 + \sqrt{Nu_{l,lam}^2 + Nu_{l,turb}^2} \quad (11)$$

$Nu_{l,lam}$ and $Nu_{l,turb}$ can be obtained with Equations (12) and (13).

$$Nu_{l,lam} = 0.664.\sqrt{\mathrm{Re}}.\sqrt{\mathrm{Pr}} \quad (12)$$

$$Nu_{l,turb} = \frac{0.037.\mathrm{Re}^{0.8}.\mathrm{Pr}}{1 + 2.443.\mathrm{Re}^{-0.1}.(\mathrm{Pr}^{2/3} - 1)} \quad (13)$$

The velocity in the Reynolds number in this restricted channel is determined by Equation (14).

$$w = \frac{w_0}{\psi} \quad (14)$$

where w_0 denotes the free stream velocity. The correction factor *y* is calculated by Equation (15), where *h* represents the height of the channel.

$$\psi = 1 - \frac{\pi.d_0}{4.h} \quad (15)$$

The last scenario investigated is the flow via tube bundle. The prototype has just one row of twenty-five tubes; hence, it cannot be termed a standard tube bundle. Therefore, the distance between the row of tubes, the wall, and the free surface of the water will be used in this scenario. Equation (16) determines the Nusselt number.

$$Nu_{0,bundle} = f_A.Nu_{l,0} \quad (16)$$

Equation (17) calculates the factor f_A for an in-line tube arrangement.

$$f_A = 1 + \frac{0.7\,(b/a - 0.3)}{\psi_b^{1.5}.(b/a - 0.7)^2} \quad (17)$$

$Nu_{l,0}$ is calculated with Equation (11). The Reynolds number is calculated using Equation (18).

$$\mathrm{Re} = \frac{w.l}{\psi_b.\nu} \quad (18)$$

y_b is computed by Equation (19) if $b \geq 1$ and by Equation (20) if $b < 1$. *a* is obtained with Equation (21), and *b* with Equation (22). s_1, s_2, and d_o stand for the distance between tubes in the cross direction, the distance between tubes in the flow direction, and the diameter of the tubes, respectively.

$$\psi_b = 1 - \frac{\pi}{4.a} \quad (19)$$

$$\psi_b = 1 - \frac{\pi}{4.a.b} \quad (20)$$

$$a = \frac{s_1}{d_0} \quad (21)$$

$$b = \frac{s_2}{d_0} \quad (22)$$

These equations are valid for *Re* between 10 and 10^6 and *Pr* between 0.6 and 1000 [29].

2.2. CFD Model of Heat Exchanger

2.2.1. Geometry

To simulate the hot water flow within the prototype, some simplifications were made. The entrance and leaving of hot water were simplified by eliminating the circular section and focusing exclusively on the rectangular component of the

heat exchanger. Furthermore, the rectangular part of the heat exchanger is not entirely filled with hot water; hence, the air is repressed, and the top surface is considered a moving wall with a velocity equal to the water's average speed. It is assumed that water circulates 2 millimeters above the tubes. Finally, the elbow geometry was simplified, as shown in Figure 2.

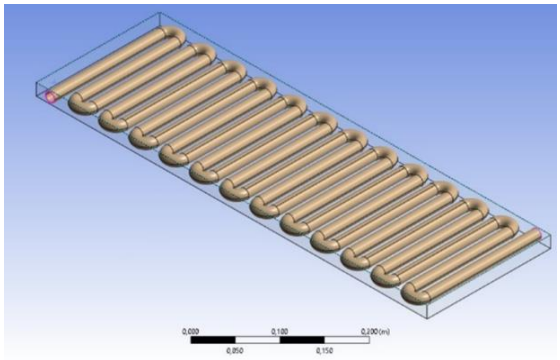

Fig. 2. Heat exchanger geometry used in the CFD model

Given the prototype's thick plastic elbows with low thermal conductivity, heat transfer via the elbows was assumed to be negligible.

2.2.2. Mesh and Models

A mesh quality analysis was carried out prior to running a CFD simulation. Initially, a coarse mesh is used, which is then gradually improved by adding more and smaller components, particularly near walls where gradients are stronger. A coarser mesh that produces adequate results is chosen. This method optimizes computing resources and saves time for future simulations [31].

Regarding models, to study thermal performance, the energy equation needs to be considered alongside the viscous model. For the cold-water flow inside the tubes, turbulence is observed for all the studied flow rates, and thus, a suitable turbulence model needs to be selected. The *k-e* turbulence model is widely used in literature, and the *k-e* realizable model has been identified as the most effective for this type of study, so this is the selected model [32].

2.2.3. Twisted Tape

The twisted tape was selected as the heat transfer enhancement device mainly because of its low cost and simplicity [33]. Figure 3 shows the model's geometry, with the width of the twisted tape about equal to the tube diameter. To avoid exceedingly narrow gaps during simulations, two fluid volumes are generated: one above and one below the tape. The study's primary goal is to determine the ideal shape; hence, just a straight tube supplied with twisted tape is modeled, rather than the whole array of tubes seen in the prototype. The best twisted tape for the prototype will also work well for a straight tube. The length of the tube used in the simulations varied between 10 cm and 100 cm. The upper limit was selected after the fluctuations in the relevant parameters, such as the Nu number and the friction factor, were no longer affected.

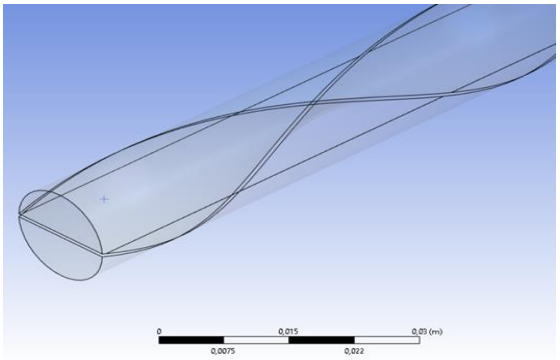

Fig. 3. Geometry of the twisted tape used in the CFD model

To simulate the impact of the hot shower water around the tube, a boundary condition of 10000 W/m^2 for the heat flux supplied to the tube wall for heating the cold water is defined based on the average conditions of the heat exchanger prototype. The twisted tape is considered adiabatic. The energy equation is used, and the turbulence *k-e* realizable model is used along with the *k-e* RNG and *k-ω* SST models [18, 34-36].

Simulations in ANSYS Fluent provide the heat transfer coefficient (h_i) used to determine the Nusselt number using Equation (23). The friction factor (f) and Nusselt number are not derived directly from ANSYS Fluent. The friction factor is computed employing the Darcy-Weisbach equation (Equation (24)) and taking the pressure difference (Δp) between the intake and exit of the tube from the CFD simulation results. The friction factor is calculated using the pipe diameter d_i, water density ρ, simulation tube length l, and fluid average velocity [30].

$$Nu = \frac{h_i . d_i}{\lambda} \tag{23}$$

$$f = \frac{2 . \Delta p . d_i}{\rho . l . w_t^2} \tag{24}$$

Equation (25) uses the friction factor and Nusselt number to get the thermal performance factor. To compute it, an empty tube simulation is run with the same turbulence model and flow rate. This simulation calculates the friction factor (f_0) and Nusselt number (Nu_0) in the absence of twisted tape.

$$\eta = \frac{Nu / Nu_0}{(f / f_0)^{1/3}} \tag{25}$$

The major aim is to find a twisted tape that can raise the Nusselt number without considerably affecting the thermal performance factor while maintaining the pressure loss. To optimize the geometry of the twisted tape, several tape twist ratios (Y) and thicknesses (δ) are simulated. Once these values are determined, the thermal performance factor of the tape will be evaluated at various water flow rates. The tape twist ratio is defined as the ratio between the length of a 180º rotation of the tape and the tube's inner diameter.

The validation of the results produced from the CFD simulations and comparisons will be done using literature correlations. Because the flow is turbulent, the use of turbulent flow correlations is required. Nusselt numbers are determined using the Equations (26) and (27) [37]. The Nusselt number for a tape without any twist ($Nu_{y=\infty}$) is calculated using Equation (26), where δ and d denote the tape thickness and diameter, respectively. Equation (27) will be used to calculate the Nusselt number for the case without any twist, $Nu/Nu_{y=\infty}$.

$$Nu_{y=\infty} = 0.023 \cdot \mathrm{Re}^{0.8} \cdot \mathrm{Pr}^{0.4} \cdot \left(\frac{\pi}{\pi - 4\delta/d} \right)^{0.8} \cdot \left(\frac{\pi + 2 - 2\delta/d}{\pi - 4\delta/d} \right)^{0.2} \quad (26)$$

$$\frac{Nu}{Nu_{y=\infty}} = 1 + \frac{0.769}{Y} \quad (27)$$

The friction factor will be calculated using Equation (28) [37]. This equation considers both the Reynolds number, as well as the dimensions of the tape, expressed by δ and d. The friction factor will be calculated considering the influence of the tape on fluid flow using the twist ratio (Y).

$$f = \frac{0.0791}{\mathrm{Re}^{0.25}} \cdot \left(\frac{\pi}{\pi - 4\delta/d} \right)^{1.75} \cdot \left(\frac{\pi + 2 - 2\delta/d}{\pi - 4\delta/d} \right)^{1.25} \cdot \left(1 + \frac{2.752}{Y^{1.29}} \right) \quad (28)$$

3. Results and Discussion

Before conducting simulations to identify the optimal twisted tape geometry, a mesh analysis was undertaken to determine the most effective mesh, a tube length study was conducted to identify the appropriate tube length, and a twisted ratio study to maximize the thermal performance factor. These simulations employed a flow rate of 9.2 L/min.

3.1. Theoretical Model Validation

Figure 4 shows the heat exchanger's effectiveness at various flow rates. These effectiveness are derived from a comprehensive range of literature correlations and experimental data of E. A. Silva [38]. Regarding literature correlations, the internal convection coefficient is determined by averaging the valid correlations among the three presented in subsection 2.2.1. The outside convection coefficient is calculated using various correlations described in paragraph 2.2.2, resulting in innovative models. While Model 2 utilizes the correlation for crossflow around a cylinder, Model 1 uses it for crossflow around a cylinder in a restricted channel. Model 3 uses the correlation for the convection coefficient on a bundle of tubes. Model 4 uses the average of the convection coefficients used in Models 1 and 2.

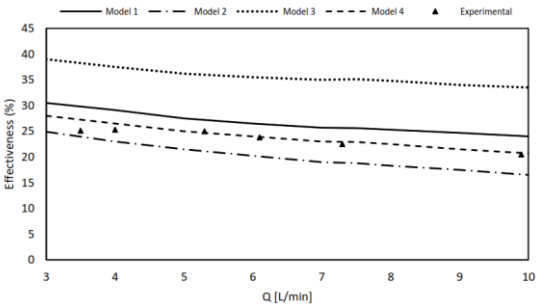

Fig. 4. Heat exchanger effectiveness results

Figure 4 shows that Model 4 has the highest agreement with the experimental data of E.A. Silva [38], with deviations ranging from 7.32% to 0.82%.

3.2. Mesh Study

Figure 5 shows the results of the mesh sensitivity analysis, which examined how mesh refinement affects the estimated Nusselt number and friction factor. The findings were obtained using the k-e realizable turbulence model for a 500 mm tube with a twist ratio of 4.

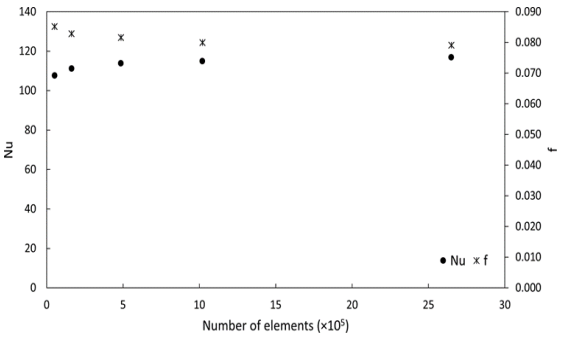

Fig. 5. Variation of the Nusselt number with the number of elements in the mesh

Figure 5 demonstrates that the Nusselt number and friction factor show very minimal fluctuations beyond the third point, corresponding to a mesh size of 486132 elements. The percentage discrepancies detected

in reference to the point with the maximum number of items (2649234) were 2.56% and 3.14%, respectively. As a result, the mesh configuration corresponding to the third point, which uses a general element size of 2.5 mm and 1 mm along the walls, may be regarded as a reliable alternative.

3.3. Tube Length Study

Figure 6 shows the simulation findings for the influence of tube length change. These results were obtained using the k-ω SST turbulence model, previously calculated mesh parameters, and a twist ratio of 4.

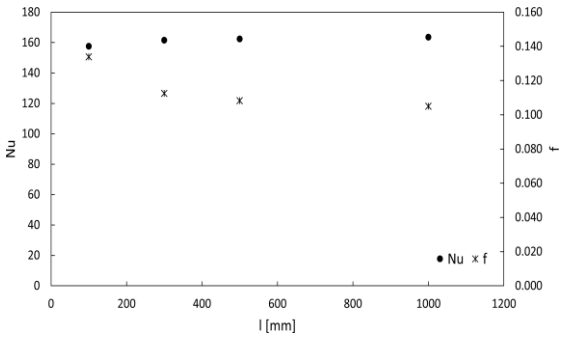

Fig. 6. Variation of the Nusselt number and friction factor with the length of the tube

After evaluating the supplied findings, differences in the Nusselt number and friction factor are insignificant beyond the third point (500 mm). Beyond this point, the Nusselt number and friction factor only changed by 0.68% and 3.04%, respectively. As a result, a tube length of 500 mm is judged appropriate for evaluating the performance of various twisted tapes.

3.4. CFD Twisted Tape Study

Figure 7 shows streamline coming from the tube intake, demonstrating the rotating flow induced by the twisted tape. This rotating flow meets expectations and adds to the improvement of the heat transfer coefficient.

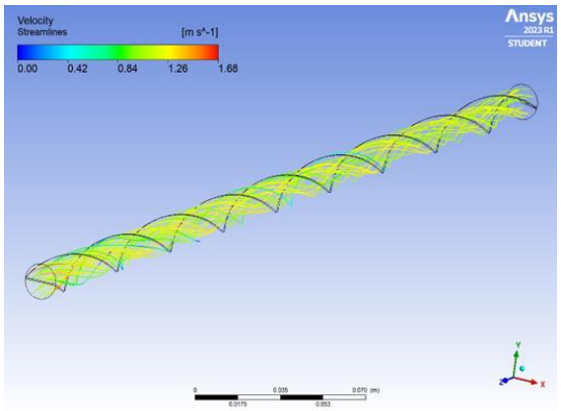

Fig. 7. Streamlines of the flow

The influence of the twist ratio (Y) is investigated while the tape thickness remains constant at 0.5 mm. Figures 8 to 10 illustrate how the twist ratio affects the Nusselt number, friction factor, and thermal performance factor. In addition, the Nusselt number and friction factor figures for a simple tube without twisted tape are shown. These values are derived using the Dittus-Boelter and Darcy-Weisbach equations, respectively, and are denoted as "correlation" in Figures 8-13.

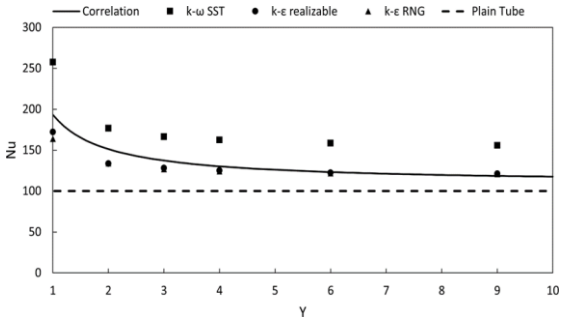

Fig. 8. Variation of the Nusselt number with the twist ratio (δ = 0.5 mm)

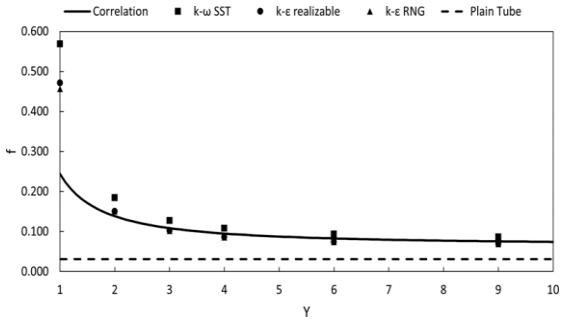

Fig. 9. Variation of the friction factor with the twist ratio (δ = 0.5 mm)

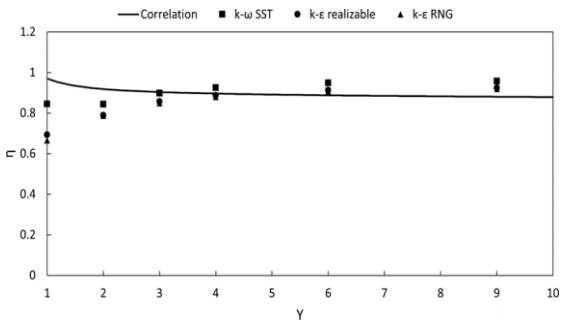

Fig. 10. Variation of the thermal performance factor with the twist ratio (δ = 0.5 mm)

The results demonstrate that when the twist ratio drops, both the Nusselt number and the friction factor rise, which is to be expected given that it improves the heat transfer coefficient but also increases pressure drop. When compared to the correlation of Dittus-Boelter and Darcy-Weisbach, the *k-ε* models exhibit better agreement, with discrepancies in the Nusselt number generally less than 10%, whereas the *k-ω* model overpredicts the data by 17 to 33%.

All models exhibit excellent agreement with the correlation of Dittus-Boelter and Darcy-Weisbach for friction factor, with discrepancies of approximately 10%, except for the lower twist ratios (1 and 2), where the model predicts a substantially greater friction factor. This can be attributable to the scarcity of theoretical data on these twist ratios, as most of the data is based on twist ratios equal to or greater than 3. This difference in friction factors at lower twist ratios also explains the lower thermal performance factor. Figure 12 demonstrates that the thermal performance factor falls significantly below a twist ratio of 3.

After examining the data, it was established that a twist ratio of 4 results in a considerable rise in the Nusselt number while not significantly compromising the thermal performance factor. As a result, this twist ratio is picked as the optimal value. Figures 11 to 13 demonstrate how tape thickness affects the Nusselt number, friction factor, and thermal performance factor. This was tested on twisted tape with a twist ratio of 4.

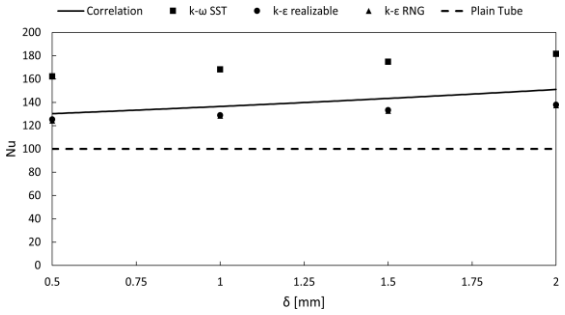

Fig. 11. Variation of the Nusselt number with the tape thickness

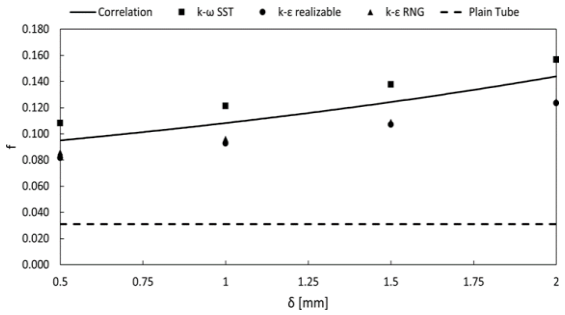

Fig. 12. Variation of the friction factor with the tape thickness

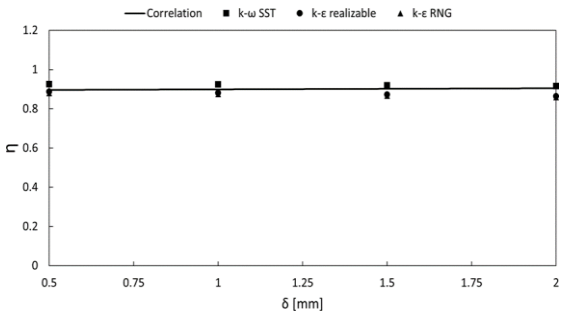

Fig. 13. Variation of the thermal performance factor with the tape thickness

Figures 11 and 12 show that increasing tape thickness increases both the Nusselt number and the friction factor. Figure 13 shows that as tape thickness rises, the thermal performance factor decreases slightly. As a result, a 1 mm tape thickness is found to be a good balance between improved heat transfer as demonstrated in Figure 13, influence on pressure drop as demonstrated in Figure 12 through the friction factor, and material cost since a reduced thickness represents a smaller amount of material.

3.5. Heat Exchanger with Twisted Tapes

The convection coefficient is calculated from the CFD simulations of the individual twisted tapes and used to replace the inner convection coefficient to account for the impacts of the twisted tapes (TT). Figure 14 shows the heat exchanger effectiveness results when the twisted tape is used vs. without resorting to model 4. The selected twisted tape has a twist ratio of four and a thickness of one millimeter.

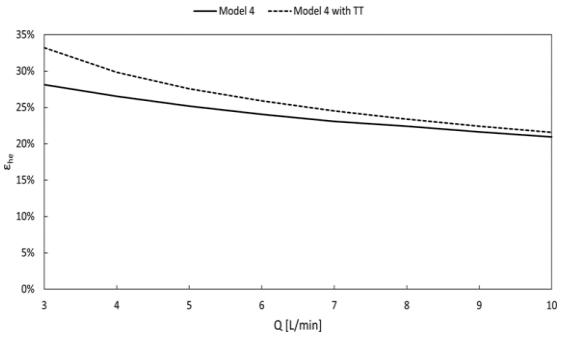

Fig. 14. Heat exchanger effectiveness with and without twisted tape

According to [39, 40], twisted tape has a greater influence in the thermal performance at lower flow rates. When the flow inside the tubes reaches a fully turbulent condition (usually at volume flow rates greater than 7.5 L/min, corresponding to Reynolds numbers above 10000), the addition of the twisted tape does not significantly increase the convection coefficient.

Given that the average flow rate of an American shower is approximately 7.9 L/min [27], and the European Commission [26] specifies that maximum flow rates for showerheads in EU Member States range from 8 to 12 L/min, if the shower flow rate falls within these upper limits, the addition of twisted tape to the prototype may have no effect. However, several shower-heads are especially intended to work at flow rates of around 5 L/min [41]. In such cases, integrating the twisted tape can raise effectiveness by 9.55%, compared to a 4.32% improvement at an 8 L/min flow rate.

4. Conclusions

The objective of this work was to offer a CFD model and a theoretical model to evaluate the performance of a shower water horizontal heat exchanger with twisted tape inserts. The theoretical and CFD models were validated against experimental data from the literature. To increase the heat exchanger's effectiveness, a thorough analysis was done using the CFD model to establish the best shape of a twisted tape insert.

Results of the theoretical models show that the convection coefficient of the shower horizontal heat exchanger falls between the cases of flow around a cylinder (Model 2) and flow around a cylinder in a narrow channel (Model 1). Averaging the convection coefficients (Model 4) results in better agreement with the experimental data. A conclusion is drawn that Model 4 represents a good approximation of our heat exchanger prototype's exterior convection coefficient.

The CFD results for twisted tape inserts are in good agreement with theoretical data, except for twist ratios of less than 3, which are rarely discussed in the literature. The main outcomes of the CFD model for twisted tape inserts are:

- Nusselt number and friction factor rise as the twist ratio decreases and tape thickness increases.
- Thermal performance factor begins to drop for twist ratios below 3.
- Thermal performance factor remains virtually constant as tape thickness varies.
- The most acceptable thickness for twisted tape is 1 mm with a twist ratio of 4. This arrangement achieves a good compromise between improving heat transfer, reducing pressure loss, and maximizing material use.
- Lower flow rates had a greater influence on the thermal performance factor of the twisted tape. When the flow gets totally turbulent, the tape's impact diminishes.
- The effect of twisted tape on heat exchanger performance is more pronounced at lower flow rates.
- Installing twisted tape in water-saving showerheads with a flow rate of 5 L/min improves heat exchanger performance by 9.55%. However, flow rates closer to the American average of 8 L/min show a 4.32% improvement.

The main contribution of this work is that it showed that the convection coefficient on the inside of the tubes with twisted tapes is higher than that on the outside. Therefore, further developments to improve the heat transfer in horizontal heat exchangers should aim to increase the outside convection heat transfer coefficient.

Nomenclature

a	Bundle transverse spacing factor
A_{ht}	Area of heat transfer [m^2]
A_i	Internal area of heat transfer [m^2]
A_o	Outside area of heat transfer [m^2]
A_t	Transverse area of the flow [m^2]
b	Bundle longitudinal spacing factor
b_{shell}	Inner base of the shell [m]
$c_{p,c}$	Specific heat of cold water [J/kg.K]
$c_{p,h}$	Specific heat of hot water [J/kg.K]
d	Tape width or diameter [m]
d_i	Tube inner diameter [m]
d_{elbow}	Diameter of the semi-circle formed by the elbow [m]
d_o	Tube outer diameter [m]
d_w	Coiled wire winding diameter [m]
Δp	Pressure loss between inlet and outlet [Pa]
Δp_{plain}	Pressure loss between inlet and outlet on a plain tube [Pa]
DT_{lm}	Log mean temperature difference [K]
DT_m	Mean temperature difference [K]
d	Tape thickness [m]
E	Energy [J/kg]
e_w	Coiled wire diameter [m]
ϵ	Turbulent dissipation rate [m^2/s^3]
ϵ_{he}	Heat exchanger effectiveness
ϵ_r	Equivalent roughness [m]
F	Body force vector per unit volume [N/m^3]
f	Friction factor
f_0	Friction factor without enhancing device
f_A	In-line arrangement factor
f_{corrl}	Friction factor from the Darcy-Weisbach equation

f_{plain}	Friction factor on a plain tube
f	Free stream velocity correction factor
f_b	Bundle correction factor
g	Gravitational acceleration [m/s²]
H	Tape twist for a 180º rotation [m]
h	Channel height [m]
h_i	Internal convection coefficient [W/m².K]
h_j	Sensible enthalpy [J/kg]
h_o	Outside convection coefficient [W/m².K]
h_{shell}	Inner height of the shell [m]
h_{plain}	Convection coefficient on a plain tube [W/m².K]
h	Thermal performance factor
I	Unit tensor
J_j	Diffusion flux of species j [kg/m²s]
k	Turbulent kinetic energy [J/kg]
k_{eff}	Effective conductivity [W/m·K]
k_t	Turbulent thermal conductivity [W/m·K]
l	Tube length [m]
$l_{1,tube}$	Length of one tube [m]
l_{shell}	Inner length of the shell [m]
l	Thermal conductivity [W/m.K]
$\dot{m}_c$	Mass flow rate of cold water [kg/s]
$\dot{m}_h$	Mass flow rate of hot water [kg/s]
m	Dynamic viscosity [Pa.s]
n	Manning resistance coefficient
n_{el}	Number of elements in the mesh
Nu	Nusselt number
Nu_0	Nusselt number without enhancing device
$Nu_{0,b}$	Bundle average Nusselt number
Nu_{corrl}	Nusselt number from the Dittus-Boelter equation
$Nu_{l,0}$	Average Nusselt number
$Nu_{l,lam}$	Laminar Nusselt number
$Nu_{l,turb}$	Turbulent Nusselt number
Nu_{plain}	Nusselt number on a plain tube
$Nu_{y=\infty}$	Nusselt number for a tape without twist
n	Kinematic viscosity [m²/s]
p	Static pressure [Pa]
p_w	Coiled wire pitch [m]
Pr	Prandtl number
Q	Volume flow rate [m³/s]
$\dot{Q}_{ex}$	Heat transfer power [W]
R_h	Hydraulic diameter [m]
R_{wall}	Wall thermal resistance [K/W]
Re	Reynolds number
r	Density [kg/m³]
S_0	Slope
s_1	Transverse tube spacing [m]
s_2	Longitudinal tube spacing [m]
S_h	Heat of possible heat sources [W/m³]
S_m	Source term [kg/m³s]
t	Time [s]
T	Temperature [K]
DT_1	First temperature difference for DT_{lm} [K]
DT_2	Second temperature difference for DT_{lm} [K]
$T_{c,in}$	Inlet temperature of cold water [K]
$T_{c,out}$	Outlet temperature of cold water [K]
$T_{h,in}$	Inlet temperature of hot water [K]
$T_{h,out}$	Outlet temperature of hot water [K]
t	Stress tensor [Pa]
t_{eff}	Effective stress tensor [Pa]
U	Overall heat transfer coefficient [W/m².K]
v	Velocity vector [m/s]
x	Correlation parameter
w	Corrected free stream velocity [m/s]
w_o	Free stream velocity [m/s]
w_t	Tube water velocity [m/s]
w	Specific dissipation rate [s^{-1}]
Y	Tape twist ratio

Funding Statement

This research did not receive any specific grant from funding agencies in the public, commercial, or not-for-profit sectors.

Conflicts of Interest

The author declares that there is no conflict of interest regarding the publication of this article.

References

[1] McNabola A., Shields, K., 2013. Efficient drain water heat recovery in horizontal domestic shower drains. Energy and Buildings, 59, pp. 44–49.

[2] Ravichandran, A., Diaz-Elsayed, N., Thomas, S., Zhang, Q., 2021. An assessment of the influence of local conditions on the economic and environmental sustainability of drain water heat recovery systems, Journal of Cleaner Production, 279, 123589.

[3] Vavřička, R., Boháč, J., Matuška, T., 2022. Experimental development of the plate shower heat exchanger to reduce the domestic hot water energy demand, Energy and Buildings, 254, 111536.

[4] Kázmierczak, B., Kordana, S., Slys, D., 2017. Analysis of profitability of using a heat recovery system from grey water discharged from the shower (case study of Poland), E3S Web of Conferences, 22.

[5] Kordana-Obuch S., Starzec, M., 2022. Horizontal shower heat exchanger as an effective domestic hot water heating alternative, Energies, 15(13), 4829.

[6] Piotrowska, B., Slys, D., Kordana-Obuch, S., Pochwat, K., 2020. Critical analysis of the current state of knowledge in the field of waste heat recovery in sewage systems, Resources, 9(6) 72.

[7] Selimli S., Eljetlawi, I.A.M., 2020. The experimental study of thermal energy recovery from shower greywater, Energy Sources, Part A: Recovery, Utilization, and Environmental Effects, 43(23), pp. 3032–3044.

[8] Shields, K. 2011. Drain water heat recovery (Master Dissertation, Trinity College Dublin).

[9] Wong, L.T., Mui, K.W., Guan, Y., 2010. Shower water heat recovery in high-rise residential buildings of Hong Kong, Applied Energy, 87(2), pp. 703–709.

[10] Kordana-Obuch, S., Starzec, M., Slys, D., 2021. Assessment of the feasibility of implementing shower heat exchangers in residential buildings based on users'e saving preferences, Energies, 14(17), p. 5547.

[11] Deng, Z., Mol, S., van der Hoek, J.P., 2016. Shower heat exchanger: reuse of energy from heated drinking water for CO_2 reduction, Drinking Water Engineering and Science, 9(1), pp. 1–8.

[12] Slys D., Kordana, S., 2014. Financial analysis of the implementation of a drain water heat recovery unit in residential housing, Energy and Buildings, 71, pp. 1–11.

[13] Shijie, L., Zuoqin, Q., Qiang, W., 2023. Optimization of thermohydraulic performance of tube heat exchanger with L twisted tape, International Communications in Heat and Mass Transfer, 145, p. 106 842.

[14] Varun, Garg, M.O., Nautiyal, H., Khurana, S., Shukla, M.K., 2016. Heat transfer augmentation using twisted tape inserts: A review, Renewable and Sustainable Energy Reviews, 63, pp. 193–225.

[15] Patil S., Babu, P., 2011. Heat transfer augmentation in a circular tube and square duct fitted with swirl flow generators: A review," International Journal of Chemical Engineering and Applications, 2, pp. 326–331.

[16] Sarma, P.K., Subramanyam, T., Kishore, P.S., Rao, V.D., Kakac, S., Laminar convective heat transfer with twisted tape inserts in a tube, 2003, International Journal of Thermal Sciences, 42(9), pp. 821–828.

[17] Sarma, P.K., Kishore, P.S., Rao, V.D., Subrahmanyam, T., 2005. A combined approach to predict friction coefficients and convective heat transfer characteristics in A tube with twisted tape inserts for a wide range of Re and Pr, International Journal of Thermal Sciences, 44(4), pp. 393–398.

[18] Yadav, A.S., Shrivastava, V., Sharma, A., Sharma, S.K., Dwivedi, M.K., Shukla, O.P., 2021. CFD simulation on thermo-hydraulic

characteristics of a circular tube having twisted tape inserts, Materials Today: Proceedings, 47, pp. 2790–2795.

[19] Yadav, A.S., Shrivastava, V., Dwivedi, M.K., Shukla, O.P., 2021. 3-dimensional CFD simulation and correlation development for circular tube equipped with twisted tape, Materials Today: Proceedings, 47, pp. 2662–2668.

[20] Shabanian, S.R., Rahimi, M., Shahhosseini, M., Alsairafi, A.A., 2011. CFD and experimental studies on heat transfer enhancement in an air cooler equipped with different tube inserts, International Communications in Heat and Mass Transfer, 38(3), pp. 383–390.

[21] Wang, Y., Hou, M., Deng, X., Li, L., Huang, C., Huang, H., Zhang, G., Chen, C., Huang, W., 2011. Configuration optimization of regularly spaced short-length twisted tape in a circular tube to enhance turbulent heat transfer using CFD modeling, Applied Thermal Engineering, 31(6), pp. 1141–1149.

[22] Jayranaiwachira, N., Promvonge, P., Thianpong, C., Skullong, S., 2023. Entropy generation and thermal performance of tubular heat exchanger fitted with louvered corner-curved V-baffles, International Journal of Heat and Mass Transfer, 201, p. 123638.

[23] Wang, J., Zeng, L., He, Y., Zhao, B., Chu, P., 2024. Effect of structure parameters on thermal performance of novel punched V-shape VGs for hear exchangers: An experimental approach. International Communications in Heat and Mass Transfer, 155, p. 107472.

[24] Nakhchi, M.E., Esfahani, J.A., 2019. Sensitivity analysis of a heat exchanger tube fitted with cross-cut Twisted Tape with Alternate Axis. J. Journal of Heat Transfer, 141(4), p. 041902.

[25] NEN 7120:2011: Energy performance of buildings - Determination method, 2011.

[26] Kaps R., Wolf, O., 2011. Development of European ecolabel and green public procurement criteria for sanitary tapware - Taps and showerheads, European Commission, Tech. Rep.

[27] De Oreo, W.B., Mayer, P.W., Dziegielwski, B., Kiefer, J.C., 2016. Residential Uses of Water 2016, Water Research Foundation, Tech. Rep..

[28] Bergman, T.L., Lavine, A.S., Incropera, F.P., DeWitt, D.P., 2017. Fundamentals of Heat and Mass Transfer. Wiley.

[29] Gnielinski, V., 2010. VDI Heat Atlas, in 2nd ed. Springer, pp. 714–775.

[30] Gerhart, P.M., Gerhart, A.L., Hochstein, J.I., 2026. Fundamentals of Fluid Mechanics, 8th ed. Wiley.

[31] Ferziger J., Peric, M., 2001. Computational Methods for Fluid Dynamics, Springer Berlin Heidelberg.

[32] Ozden E., Tari, I., 2010. Shell side CFD analysis of a small shell-and-tube heat exchanger, Energy Conversion and Management, 51(5), pp. 1004–1014.

[33] García, A., Solano, J.P., Vicente, P.G., Viedma, A., 2007. Enhancement of laminar and transitional flow heat transfer in tubes by means of wire coil inserts, International Journal of Heat and Mass Transfer, 50(15-16), pp. 3176–3189.

[34] Eiamsaard, S., Wongcharee, K., Sripattanapipat, S., 2009. 3-D Numerical simulation of swirling flow and convective heat transfer in a circular tube induced by means of loose-fit twisted tapes, International Communications in Heat and Mass Transfer, 36(9), pp. 947–955.

[35] Kaliakatsos, D., Cucumo, M., Ferraro, V., Mele, M., Galloro, A., Accorinti, F., 2016. CFD analysis of a pipe equipped with twisted tape, International Journal of Heat and Technology, 34(2), pp. 172–180.

[36] Rahimi, M., Shabanian, S.R., Alsairafi, A.A., 2009. Experimental and CFD studies on heat transfer and friction factor characteristics of a tube equipped with modified twisted tape inserts, Chemical Engineering and Processing: Process Intensification, 48(3), pp. 762–770.

[37] Manglik R.M., Bergles, A.E., 1993. Heat transfer and pressure drop correlations for twisted-tape inserts in isothermal tubes: Part II—Transition and turbulent flows, Journal of Heat Transfer, 115(4), pp. 890–896.

[38] Silva, E.A. 2023. Optimization of heat transfer in a shower water heat exchanger (Master Dissertation, University of Porto). Available at: https://repositorio-aberto.up.pt/bitstream/10216/151449/2/635868.pdf.

[39] Maradiya, C., Vadher, J., Agarwal, R., 2018. The heat transfer enhancement techniques and their thermal performance factor, Beni-Suef University Journal of Basic and Applied Sciences, 7(1), pp. 1–21.

[40] Shelare, S.D., Aglawe, K.R., Belkhode, P.N., 2022. A review on twisted tape inserts for enhancing the heat transfer, Materials Today: Proceedings, 54, pp. 560– 565.

[41] DECO Proteste, Poupe água com os hábitos e os dispositivos certos, Accessed at 20-05-2023, 2023. [Online]. Available: https://www.deco.proteste.pt/casa-energia/agua/noticias/poupe-agua-habitos-dispositivos-certos.